

Notice that the interface block structure of MRAS does *not* match the one in [3, Algorithm 2] but the transmission matrix D is chosen to get fast convergence, analogously to the parameter p in POSM. Setting

$$\begin{aligned} E_{\Gamma_2}^{\Omega_1} &:= [0_{\Theta_1} I_{\Gamma_2} 0_O 0_{\Gamma_1}]^T, & E_{\Gamma_1}^{\Omega_1} &:= [0_{\Theta_1} 0_{\Gamma_2} 0_O I_{\Gamma_1}]^T, & E_{\Theta_1}^{\Omega_1} &:= [A_{\Gamma_2, \Theta_1} 0_{\Gamma_2} 0_O 0_{\Gamma_1}]^T, \\ E_{\Gamma_2}^{\Omega_2} &:= [I_{\Gamma_2} 0_O 0_{\Gamma_1} 0_{\Theta_2}]^T, & E_{\Gamma_1}^{\Omega_2} &:= [0_{\Gamma_2} 0_O I_{\Gamma_1} 0_{\Theta_2}]^T, & E_{\Theta_2}^{\Omega_2} &:= [0_{\Gamma_2} 0_O 0_{\Gamma_1} A_{\Theta_2, \Gamma_1}]^T, \end{aligned}$$

we can write

$$\tilde{A}_{\Omega_i} = A_{\Omega_i} + E_{\Gamma_i}^{\Omega_i} D \left(E_{\Gamma_i}^{\Omega_i} \right)^T, \quad i = 1, 2,$$

and formulate a convergence result for MRAS, analogue to [2, Theorem 3.2].

Theorem 1 ([2, Section 3])

The MRAS iteration matrix T in (5) has the structure

$$T = \begin{bmatrix} 0 & K \\ L & 0 \end{bmatrix}, \quad \begin{aligned} K &:= A_{\Omega_1}^{-1} E_{\Gamma_1}^{\Omega_1} \left[I + D(A_{\Omega_1}^{-1})_{\Gamma_1, \Gamma_1} \right]^{-1} \left(-D(E_{\Gamma_1}^{\Omega_2})^T + (E_{\Theta_2}^{\Omega_2})^T \right), \\ L &:= A_{\Omega_2}^{-1} E_{\Gamma_2}^{\Omega_2} \left[I + D(A_{\Omega_2}^{-1})_{\Gamma_2, \Gamma_2} \right]^{-1} \left(-D(E_{\Gamma_2}^{\Omega_1})^T + (E_{\Theta_1}^{\Omega_1})^T \right). \end{aligned} \quad (6)$$

Moreover, the asymptotic convergence factor of MRAS is bounded by

$$\begin{aligned} &\sqrt{\|M_1 B_1\|_2 \cdot \|M_2 B_2\|_2}, \\ M_1 &:= \left[I + D(A_{\Omega_1}^{-1})_{\Gamma_1, \Gamma_1} \right]^{-1} \left(-D - A_{\Gamma_1, \Theta_2} A_{\Theta_2}^{-1} A_{\Theta_2, \Gamma_1} \right), \quad B_1 := (A_{\Omega_2}^{-1})_{\Gamma_1, \Gamma_2}, \\ M_2 &:= \left[I + D(A_{\Omega_2}^{-1})_{\Gamma_2, \Gamma_2} \right]^{-1} \left(-D - A_{\Gamma_2, \Theta_1} A_{\Theta_1}^{-1} A_{\Theta_1, \Gamma_2} \right), \quad B_2 := (A_{\Omega_1}^{-1})_{\Gamma_2, \Gamma_1}. \end{aligned} \quad (7)$$

Due to the symmetry of the model problem and the method we have $B := B_1 = B_2$ and $M := M_1 = M_2$, which in turn simplifies the bound in (7) to $\|MB\|_2$.

2 Analysis of the MRAS bound and its reformulation

First, we recall the sine series expansion in the y direction \mathcal{F}_y , so that we have

$$u(x, y) = \sum_{k=1}^{+\infty} \mathcal{F}_y u(x, k) \sin\left(\frac{k\pi}{b} y\right) \equiv \sum_{k=1}^{+\infty} \hat{u}(x, k) \sin\left(\frac{k\pi}{b} y\right),$$

with² $\mathcal{F}_y u := \int_0^b u(x, y) \sin(k\pi y/b) dy$. Next, we factor out $(A_{\Omega_1}^{-1})_{\Gamma_1, \Gamma_1}$ and $(A_{\Omega_2}^{-1})_{\Gamma_2, \Gamma_2}$ on the left from $M_{1,2}$, so that instead of (7) we focus on the asymptotically equivalent

² Using the sine series relies on the Dirichlet boundary conditions (BCs) along $\{y = 0\}$ and $\{y = b\}$ in (1); for different BCs see [4].

$$MB := \underbrace{\left[\left((A_{\Omega_1}^{-1})_{\Gamma_1, \Gamma_1} \right)^{-1} + D \right]^{-1}}_{(T^{\text{Denom}})^{-1}} \underbrace{\left(-D - A_{\Gamma_1, \Theta_2} A_{\Theta_2}^{-1} A_{\Theta_2, \Gamma_1} \right)}_{T^{\text{Numer}}} \underbrace{\left((A_{\Omega_2}^{-1})_{\Gamma_1, \Gamma_2} \left((A_{\Omega_2}^{-1})_{\Gamma_2, \Gamma_2} \right)^{-1} \right)}_{T^{\text{Over}}}. \quad (8)$$

The *key* question is whether the bound (7), which now becomes $\|MB\|$, is the discrete analogue of (3) – piece by piece. Linking each of the blocks in (8) to a discrete linear operator with a continuous counterpart, we analyze it using the Fourier series expansion. Taking $\mathbf{b} \in \mathbb{R}^{N_r-1}$ and interpolating it to a function $\gamma: \Gamma_1^h \rightarrow \mathbb{R}$, the following problems are equivalent up to the FD discretization:

$$A_{\Omega_1} \mathbf{u} = -\frac{1}{h^2} E_{\Gamma_1}^{\Omega_1} \mathbf{b} \quad \text{and} \quad \begin{aligned} \Delta u &= 0 && \text{in } \Omega_1^h, \\ u &= 0 && \text{on } \partial\Omega_1^h \setminus \Gamma_1^h, \quad \text{and} \quad u = \gamma && \text{on } \Gamma_1^h. \end{aligned} \quad (9)$$

Defining the solution operator by $\mathcal{S}_1(\gamma) = u|_{\Gamma_1}$ where u is the solution of (9), we have (up to the FD discretization) the equivalence of the linear operators $-1/h^2(A_{\Omega_1}^{-1})_{\Gamma_1, \Gamma_1}$ and \mathcal{S}_1 . To calculate \mathcal{S}_1 we expand in the y variable using \mathcal{F}_y , simplifying the continuous problem in (9) to the semi-discrete problem

$$\begin{aligned} \left(\partial_{xx} - \left(\frac{k\pi}{b} \right)^2 \right) \hat{u}(x, k) &= 0 && \text{for } x \in (-a, L/2 + h) \text{ and } k \in \mathbb{N}, \\ \hat{u}(-a, k) &= 0 && \text{and } \hat{u}(L/2 + h, k) = \hat{\gamma}(k) && \text{for } k \in \mathbb{N}, \end{aligned} \quad (10)$$

and denote by $\hat{\mathcal{S}}_1 := \mathcal{F}_y \mathcal{S}_1$ the Fourier symbol of \mathcal{S}_1 . A direct calculation yields

$$\hat{u}(x, k) = \frac{\sinh\left(\frac{k\pi}{b}(a+x)\right) \hat{\gamma}(k)}{\sinh\left(\frac{k\pi}{b}(a+L/2+h)\right)}, \quad \hat{\mathcal{S}}_1 \hat{\gamma}(k) = \frac{\sinh\left(\frac{k\pi}{b}(a+L/2)\right)}{\sinh\left(\frac{k\pi}{b}(a+L/2+h)\right)} \hat{\gamma}(k).$$

Therefore, the eigenvalues of the linear operator $-1/h^2(A_{\Omega_1}^{-1})_{\Gamma_1, \Gamma_1}$ approximate the modes $k = 1, \dots, N_r - 1$ of $\hat{\mathcal{S}}_1$ given above, as we see in Figure 2. The rest of the blocks in (8) are summarized in Table 1 and illustrated in Figure 2, see [4] for detailed calculations. We see that the approximation is very accurate for the low-frequency modes but not quite accurate for the high-frequency ones. If D diagonalizes in the same basis as the rest of the blocks and we denote its eigenvalues by $\delta_1, \dots, \delta_{N_r-1}$, then the eigenvalues of $T^{\text{Denom}}, T^{\text{Numer}}, T^{\text{Over}}$ approximate certain discrete (truncated) Fourier symbols we present in Table 2 and illustrate in Figure 3. We see that the inaccuracy on the high frequencies is still present. More importantly, comparing Table 2 with (3) shows that the contraction factor due to the domain overlap in (3) matches exactly θ_k for each k , i.e., the one due to the continuous representation of T^{Over} . However, this is clearly *not* the case for the contraction factor due to the transmission condition induced by D . The ratio η_k/ζ_k shows that choosing $\delta_k = p$ (the naive choice) is *not* the correct one (see [4] for more details) and we continue by reformulating Theorem 1 to reflect also the transmission part of (3).

Table 1 The blocks and corresponding linear operators (LO) from (8).

block	discrete LO	continuous LO	Fourier symbol
$(A_{\Omega_1}^{-1})_{\Gamma_1, \Gamma_1}$	$-\frac{1}{h^2} (A_{\Omega_1}^{-1})_{\Gamma_1, \Gamma_1}$	$\mathcal{S}_1 : \gamma \mapsto u _{\Gamma_1}$	$\hat{\mathcal{S}}_1 = \frac{\sinh(\frac{k\pi}{b}(a+L/2))}{\sinh(\frac{k\pi}{b}(a+L/2+h))}$
$A_{\Gamma_1, \Theta_2} A_{\Theta_2}^{-1} A_{\Theta_2, \Gamma_1}$	$-h^2 A_{\Gamma_1, \Theta_2} A_{\Theta_2}^{-1} A_{\Theta_2, \Gamma_1}$	$\mathcal{S}_2 : \gamma \mapsto u _{\Gamma_1}$	$\hat{\mathcal{S}}_2 = \frac{\sinh(\frac{k\pi}{b}(a-L/2-h))}{\sinh(\frac{k\pi}{b}(a-L/2))}$
$(A_{\Omega_2}^{-1})_{\Gamma_1, \Gamma_2}$	$-\frac{1}{h^2} (A_{\Omega_2}^{-1})_{\Gamma_1, \Gamma_2}$	$\mathcal{S}_3 : \gamma \mapsto u _{\Gamma_1}$	$\hat{\mathcal{S}}_3 = \frac{\sinh(\frac{k\pi}{b}(a-L/2))}{\sinh(\frac{k\pi}{b}(a+L/2+h))}$
$(A_{\Omega_2}^{-1})_{\Gamma_2, \Gamma_2}$	$-\frac{1}{h^2} (A_{\Omega_2}^{-1})_{\Gamma_2, \Gamma_2}$	$\mathcal{S}_4 : \gamma \mapsto u _{\Gamma_2}$	$\hat{\mathcal{S}}_4 = \frac{\sinh(\frac{k\pi}{b}(a+L/2))}{\sinh(\frac{k\pi}{b}(a+L/2+h))}$

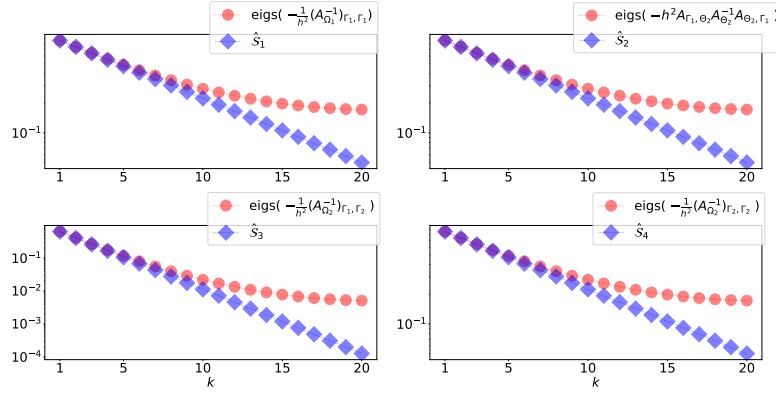

Fig. 2 Results obtained for the parameters $a = b = 1$, $L = 2h$, $N_r = 22$.

Table 2 The matrices and their corresponding (truncated) Fourier symbols.

$(\mathcal{T}^{\text{Denom}})^{-1}$	$\mathcal{T}^{\text{Numer}}$	$\mathcal{T}^{\text{Over}}$
$\eta_k := \delta_k - \frac{1}{h^2} \frac{\sinh(\frac{k\pi}{b}(a+L/2+h))}{\sinh(\frac{k\pi}{b}(a+L/2))}$	$\zeta_k := -\delta_k + \frac{1}{h^2} \frac{\sinh(\frac{k\pi}{b}(a-L/2-h))}{\sinh(\frac{k\pi}{b}(a-L/2))}$	$\theta_k := \frac{\sinh(\frac{k\pi}{b}(a-L/2))}{\sinh(\frac{k\pi}{b}(a+L/2))}$
$(\bar{\mathcal{T}}^{\text{Denom}})^{-1}$	$\bar{\mathcal{T}}^{\text{Numer}}$	$\bar{\mathcal{T}}^{\text{Over}}$
$\bar{\eta}_k := -\frac{1}{h} \frac{k\pi}{b} \coth\left(\frac{k\pi}{b}(a+L/2)\right) - \lambda_k$	$\bar{\zeta}_k := -\frac{1}{h} \frac{k\pi}{b} \coth\left(\frac{k\pi}{b}(a-L/2)\right) + \lambda_k$	$\bar{\theta}_k := \frac{\sinh(\frac{k\pi}{b}(a-L/2))}{\sinh(\frac{k\pi}{b}(a+L/2))}$

The main tool used to obtain Theorem 1 is the Sherman-Morrison-Woodbury formula for the inverse of a low-rank updated matrix, here the update was the corner block D . We now show that using the same formula for a slightly different block gives the “correct” result. We split the interface blocks as in [3, Section 5.2] and write $A_{\Gamma_1} = A_{\Gamma_1}^L + A_{\Gamma_1}^R$ and $A_{\Gamma_2} = A_{\Gamma_2}^L + A_{\Gamma_2}^R$ so that we have

$$\begin{aligned}
 -h(A_{\Gamma_1, O} \mathbf{u}_O + A_{\Gamma_1}^L \mathbf{u}_{\Gamma_1}) &\approx u_x|_{\Gamma_1}, & -h(A_{\Gamma_1, \Theta_2} \mathbf{u}_{\Theta_2} + A_{\Gamma_1}^R \mathbf{u}_{\Gamma_1}) &\approx -u_x|_{\Gamma_1}, \\
 -h(A_{\Gamma_2, O} \mathbf{u}_O + A_{\Gamma_2}^R \mathbf{u}_{\Gamma_2}) &\approx -u_x|_{\Gamma_2}, & -h(A_{\Gamma_2, \Theta_1} \mathbf{u}_{\Theta_1} + A_{\Gamma_2}^L \mathbf{u}_{\Gamma_2}) &\approx u_x|_{\Gamma_2}.
 \end{aligned} \tag{11}$$

This is natural for FD and FEM discretizations. Using the so-called *ghost point trick* we get $A_{\Gamma_1}^L = A_{\Gamma_1}^R = \frac{1}{2} A_{\Gamma_1}$, $A_{\Gamma_2}^L = A_{\Gamma_2}^R = \frac{1}{2} A_{\Gamma_2}$. Adopting this we rewrite \hat{A}_{aug} as

$$\begin{aligned} \overline{M} &:= (\overline{T}^{\text{Denom}})^{-1} \overline{T}^{\text{Numer}} = \left[\left((A_{\Omega_1}^L)^{-1} \right)_{\Gamma_1, \Gamma_1}^{-1} + \overline{A}_{\Gamma_1} \right]^{-1} \left((A_{\Gamma_1}^R - A_{\Gamma_1, \Theta_2} A_{\Theta_2}^{-1} A_{\Theta_2, \Gamma_1}) - \overline{A}_{\Gamma_1} \right), \\ \overline{B} &:= \overline{T}^{\text{Over}} = \left((A_{\Omega_2}^R)^{-1} \right)_{\Gamma_1, \Gamma_2} \left((A_{\Omega_2}^R)^{-1} \right)_{\Gamma_2, \Gamma_2}^{-1}. \end{aligned} \tag{13}$$

Focusing on the first block in (13), we take $\mathbf{b} \in \mathbb{R}^{N_r-1}$ and interpolating it to a function $\gamma: \Gamma_1 \rightarrow \mathbb{R}$, the following problems are equivalent up to the FD discretization:

$$\begin{aligned} A_{\Omega_1}^L \mathbf{u} &= -\frac{1}{h} E_{\Gamma_1}^{\Omega_1} \mathbf{b} \quad \text{and} \quad \Delta u = 0 \quad \text{in } \Omega_1, \\ u &= 0 \quad \text{on } \partial\Omega_1 \setminus \Gamma_1, \quad \text{and} \quad \mathbf{n}_1 \cdot \nabla u = \gamma \quad \text{on } \Gamma_1. \end{aligned} \tag{14}$$

Setting $\overline{\mathcal{S}}_2(\gamma) = u|_{\Gamma_1}$, where u is the solution of (14) we have the equivalence (up to the FD discretization) of $-1/h(A_{\Omega_1}^L)^{-1}_{\Gamma_1, \Gamma_1}$ and $\overline{\mathcal{S}}_2$. Considering

$$\begin{aligned} \left(\partial_{xx} - \left(\frac{k\pi}{b} \right)^2 \right) \hat{u}(x, k) &= 0 \quad \text{for } x \in (-a, L/2 + h) \text{ and } k \in \mathbb{N}, \\ \hat{u}(-a, k) &= 0 \quad \text{and} \quad \hat{u}_x(L/2 + h, k) = \hat{\gamma}(k) \quad \text{for } k \in \mathbb{N}, \end{aligned} \tag{15}$$

we set $\hat{\mathcal{S}}_1 := \mathcal{F}_y \overline{\mathcal{S}}_1$ and a direct calculation yields the solution of (15) and $\hat{\mathcal{S}}_1$ as

$$\hat{u}(x, k) = \frac{\sinh\left(\frac{k\pi}{b}(a+x)\right)}{\frac{k\pi}{b} \cosh\left(\frac{k\pi}{b}(a+L/2)\right)}, \quad \hat{\mathcal{S}}_1 \hat{\gamma}(k) = \frac{\sinh\left(\frac{k\pi}{b}(a+L/2)\right)}{\frac{k\pi}{b} \cosh\left(\frac{k\pi}{b}(a+L/2)\right)} \hat{\gamma}(k).$$

Therefore, the eigenvalues of $-1/h((A_{\Omega_1}^L)^{-1})_{\Gamma_1, \Gamma_1}$ approximate the first $N_r - 1$ modes of $\mathcal{F}_y \overline{\mathcal{S}}_1$ with better accuracy in high-frequencies than we observed with \mathcal{S}_1 , see Figure 2 and Figure 4. For the other blocks see Table 3 and Figure 4. If $-\overline{A}_{\Gamma_1}^R$ diagonalizes in the Fourier discrete basis with eigenvalues $\lambda_1, \dots, \lambda_{N_r-1}$, then the eigenvalues of $\overline{T}^{\text{Denom}}, \overline{T}^{\text{Numer}}, \overline{T}^{\text{Over}}$ approximate certain discrete (truncated) Fourier symbols, presented in Table 2 and Figure 3. Notice that at the discrete level we have $MB = \overline{MB}$, i.e., the difference is in the *representation* of the bound (blue markers in Figure 3) as we changed *only* the block organization in the Sherman-Morrison-Woodbury formula. Comparing Table 2 with (3), we get the link between λ_k (and hence also δ_k) and the Robin parameter p in (3). Calculating the optimal p now directly translates to the optimal choice of D by

$$pI = -hW^T \left(A_{\Gamma_1}^R + D \right) W \quad , \text{ i. e., } \quad D = -\frac{p}{h} I - A_{\Gamma_1}^R.$$

Table 3 The blocks and corresponding linear operators (LO) from (8).

block	discrete LO	continuous LO	Fourier symbol
$((A_{\Omega_1}^L)^{-1})_{\Gamma_1, \Gamma_1}$	$-\frac{1}{h} ((A_{\Omega_1}^L)^{-1})_{\Gamma_1, \Gamma_1}$	$\bar{S}_1 : \gamma \mapsto u _{\Gamma_1}$	$\hat{S}_1 = \frac{1}{\frac{k\pi}{b} \coth(\frac{k\pi}{b}(a+L/2))}$
$\bar{A}_{\Gamma_1}^R - A_{\Gamma_1, \Theta_2} A_{\Theta_2}^{-1} A_{\Theta_2, \Gamma_1}$	$-h (\bar{A}_{\Gamma_1}^R - A_{\Gamma_1, \Theta_2} A_{\Theta_2}^{-1} A_{\Theta_2, \Gamma_1})$	$\bar{S}_2 : \gamma \mapsto \mathbf{n}_1 \cdot \nabla u _{\Gamma_1}$	$\hat{S}_2 = \frac{k\pi}{b} \coth(\frac{k\pi}{b}(a-L/2))$
$((A_{\Omega_2}^R)^{-1})_{\Gamma_1, \Gamma_2}$	$-\frac{1}{h} ((A_{\Omega_2}^R)^{-1})_{\Gamma_1, \Gamma_2}$	$\bar{S}_3 : \gamma \mapsto u _{\Gamma_1}$	$\hat{S}_3 = \frac{\sinh(\frac{k\pi}{b}(a-L/2))}{\frac{k\pi}{b} \cosh(\frac{k\pi}{b}(a+L/2))}$
$((A_{\Omega_2}^R)^{-1})_{\Gamma_2, \Gamma_2}$	$-\frac{1}{h} ((A_{\Omega_2}^R)^{-1})_{\Gamma_2, \Gamma_2}$	$\bar{S}_4 : \gamma \mapsto u _{\Gamma_2}$	$\hat{S}_4 = \frac{\sinh(\frac{k\pi}{b}(a+L/2))}{\frac{k\pi}{b} \cosh(\frac{k\pi}{b}(a+L/2))}$

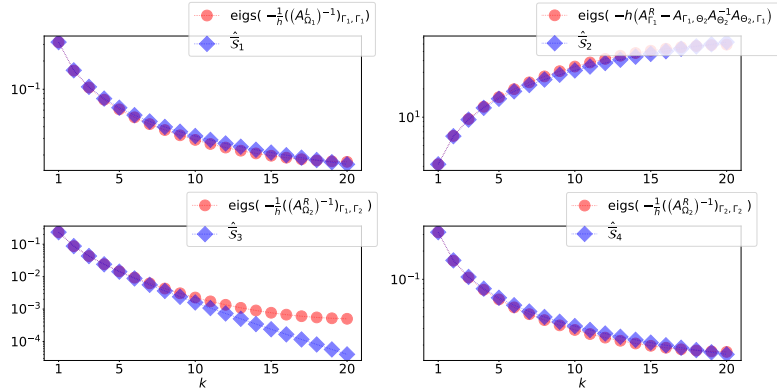


Fig. 4 Results obtained for the parameters $a = b = 1, L = 2h, N_r = 21$.

References

1. Gander, M. J. On the influence of geometry on optimized Schwarz methods. *SeMA Journal* **53**(1), 71–78 (2013).
2. Gander, M. J., Loisel, S., and Szyld, D. B. An optimal block iterative method and preconditioner for banded matrices with applications to PDEs on irregular domains. *SIAM Journal on Matrix Analysis and Applications* **33**(2), 653–680 (2012).
3. Gander, M. J. and Zhang, H. A class of iterative solvers for the Helmholtz equation: factorizations, sweeping preconditioners, source transfer, single layer potentials, polarized traces, and optimized Schwarz methods. *SIAM Review* **61**(1), 3–76 (2019).
4. Outrata, M. *Schwarz methods, Schur complements, preconditioning and numerical linear algebra*. Ph.D. thesis, University of Geneva, Math Department (2022).